ORIGINAL ARTICLE online©ML Comm
J Neurocrit Care 2008;1:31-42 ISSN 2005-0348

Tracing of Noradrenergic Neuronal Circuitry and Functional Recovery after Permanent Focal Cerebral Ischemia in Mice

Hyun-Jeong Kim, MS[1], Hyun-Woo Kim, BSc[1], Byung In Lee, MD[1], Kyoung Joo Cho, MS[1], Young Buhm Huh, MD, PhD[2] and Gyung Whan Kim, MD, PhD[1]

[1]Department of Neurology, Brain Research Institute, Yonsei University College of Medicine, Seoul, Korea
[2]Department of Anatomy, College of Medicine, Kyunghee University, Seoul, Korea

Background: Cardiovascular autonomic imbalances after stroke may be responsible for dysfunction of noradrenergic (NA) system in brain. However, exact locations or extent of NA-circuitry damage after stroke and its functional implications are remaining to be elucidated. **Methods**: Adult male C57BL/6J mice were subjected to permanent focal cerebral ischemia (pFCI) by intraluminal suture occlusion of middle cerebral artery. Recombinant adenoviral vector introducing wheat germ agglutinin (WGA)-cDNA was injected into locus coelureus (LC) using stereotaxic method. Behavioral and physiological tests were executed and immunohistochemistry for BrdU, tyrosine hydroxylase (TH), and WGA were performed at the same time. **Results**: Colocalization of GFP, TH, and WGA and restrictive expression of WGA-mRNA in LC showed that WGA protein was endogenously synthesized in NA-cells of LC. Within 6 months after pFCI onset, the extensively damaged NA-circuitry was observed in thalamic nuclei, lateral hypothalamic area, hippocampus, and amygdaloid nuclei in ipsilateral side. The damaged NA-circuits were partly reorganized over time in the area of previous lesion with the gradual recovery of autonomic dysfunction and neurobehavioral deficits. Many migrated BrdU-immunopositive cells were detected in the lesioned thalamus and hypothalamus. **Conclusion**: In this study, we successfully visualized NA-circuitries in mice by using transsynaptic tracing with PRS-WGA adenovirus. It was also confirmed the close relationships between the functional recovery and the reorganization of damaged NA-circuits. Moreover, this study demonstrated that the process of reorganization may involve axonal sprouting of intact NA-projections on newly proliferated and migrated neurons to the infarct area. **J Neurocrit Care 2008;1:31-42**

KEY WORDS: Cerebral ischemia · Norepinephrine · Wheat germ agglutinins · Genetic vector · Neuronal plasticity.

Introduction

Cardiac complications including sudden death, arrhythmia or myocardial damage are frequent during recovery phase after stroke.[1] In addition, plasma noradrenaline (NA) levels are often elevated,[2] which may be responsible for increased serum cardiac enzyme, tachycardia and high cardiac output, and high blood pressure.[3] Experimentally, plasma level of NA was significantly elevated compared to that of preocclusion condition after permanent occlusion of left middle cerebral artery (MCA) in cat.[4] Dysfunction of the noradrenergic system is a frequent feature in various neurodegenerative disorders such as Alzheimer's disease, Parkinson disease, multisystem atrophy as well as in acute ischemic stroke. Defects in the noradrenergic system have also been implicated in many psychiatric disorders manifesting abnormal social behavior, attention deficit, hyperactivity, anxiety, and depression. NA is the neurotransmitter being implicated in many of these disorders and has been found to affect social behavior in both humans and animals.[5,6] Therefore, investigating alterations of NA systems in stroke may provide clues to understand its symptomology, clinical courses, and adequate management.

Locations and size of stroke may be related to different characteristics of autonomic dysfunction.[7] The most important control sites of autonomic function are found to be the insular cortex, amygdala, and lateral hypothalamus and, among these, insular cortex and amygdala are supplied by seem MCA and play a crucial role in cardiovascular regulation.[3,8,9] Brain ischemia induces both pathological synaptic plasticity causing delayed neuronal death and induce physiological plasticity, leading structural reorganization result-

Address for correspondence: Gyung Whan Kim, MD, PhD
Department of Neurology, College of Medicine, Yonsei University, 134 Sinchon-dong, Seodaemun-gu, Seoul 120-752, Korea
Tel: +82-2-2228-2010, Fax: +82-2-393-0705
E-mail: gyungkim@yuhs.ac

This work was supported by Yonsei University Research Fund of 2006 (6-2007-0118).

ing in functional recovery.[10,11]

The wiring patterns of various neuronal populations connected by specific synaptic connections are the basis of functional logic for information processing employed by brain. To accurately identify patterns of neuronal connectivity, various neuroanatomical tracers have been used for labeling axons and dendrites of specific neurons projecting to their synaptic partner neurons.[12-14]

Plant lectins have been widely used as highly sensitive tracers in anatomical studies for mapping central neural pathways.[15,16] Among various plant lectins, WGA has been extensively studied and proved to be most efficiently transferred by projecting neurons.[17] The WGA protein injection method had been used to visualize optic pathways[18] in monkeys, olfactory systems[16] in rodents, common afferent projections to locus coelureus (LC)[19] in rat, and connections of the A5 noradrenergic cell group[20] in rat. However, the potential problem of direct injection method is hampered by its neuronal non-specificity causing all neurons located at the injection site to take up WGA protein resulting in labeling of unrelated pathways.[12,13] Recently, a novel genetic strategy employing cDNA for WGA as a transgene under the control of specific promoter elements, was introduced in neural tracing study. Studies using the genetic method were successfully conducted in transgenic mice to visualize optic pathways,[21] cerebellar efferent pathway,[14] and taste neuronal circuitries for bitter and sweet.[22] The use of WGA-expressing adenoviral vector system for visualization of neural circuitries were further expanded to a wide range of hosts, which were transferred genes in time- and place-specific manners, including the tracing of olfactory pathway in mouse[12] and the remodeling of intraspinal or cortical circuitries with functional recovery after spinal cord injury.[13,23]

This study was conducted to visualize noradrenergic neuronal circuitry using a novel genetic tracing method and to investigate the temporal relationships between the alteration of noradrenergic circuitries and functional recovery after pFCI in mice.

Materials and Methods

Focal cerebral ischemia

Adult male C57BL/6 mice (22−27g; Orient Co., Kyonggido, South Korea) were housed in a 12 h light/dark cycle and permitted food and water. These mice were anesthetized by inhalation of isoflurane in N_2O/O_2 (70 : 30%) and subjected to pFCI by MCA blockade with a 5.0 surgical monofilament nylon suture. At the end of surgery, the nylon suture was tightly fixed at the final position with a silk suture. A Laser Doppler flowmeter (transonic system Inc., New York, USA) with the probe placed directly on the skull surface over the territory of the MCA (1 mm posterior and 5 mm lateral to bregma), measured regional CBF before and after occlusion and immediately before sacrifice. Cannulation of a femoral artery allowed the monitoring of blood pressure with Pressure Transducer (Harvard Apparatus, Inc., Holliston, MA, USA). All procedures were approved by the animal care committee at Yonsei University medical college.

Infarct size measurement

Seven serial 40 μm thick slice coronal sections from each brain were cut at 800 μm intervals beginning at 2 mm from the front using a cryostat. Each slice was stained with cresyl violet. Infarct sizes were expressed as contralateral hemisphere (mm^3) minus undamaged ipsilateral hemisphere (mm^3) to correct for brain edema.[24]

Recombinant adenoviral construction and viral infection

The procedure for generation of recombinant adenoviruses was described previously.[25] The PRS-WGA adenovirus was friendly gifted from Dr. Huh, Kyunghee University. A gene cassette containing the WGA gene downstream of the PRS2x8 promoter was inserted into the pAdTrack plasmid and finally into the pAdEasy1. Recombinant adenoviral DNA was cut with Pac1 and transfected into HEK293 cells using Lipofectamine (Invitrogen, California, USA). Viruses were harvested 5 days after transfection from the transfected HEK 293 cells and amplified on dishes. The viral particles were purified by cesium chloride density gradient ultracentrifugation, dialyzed, and tittered.

Animals were anesthetized and placed in a stereotaxic instrument. After incision of the skin, a small burr hole was made directly at coordinates of LC (5.4 mm posterior, 1.0 mm lateral, and 3.8 mm deep to bregma) and the viral vector was unilaterally injected into the LC of ischemic hemisphere using a Hamilton syringe (Hamilton Co., Nevada, USA). A single injection of 0.2−0.3 μl of the concentrated adenovirus suspension (about 2×10^{13} cfu/ml) was used in this study. The scalp was then sutured, and, after the mouse was returned to standard housing. After 2 days of virus injection, mice were perfused with 4% formaldehyde and the brains were removed for histological analysis

Immunohistochemistry

Fixed mouse brains were cut with a cryostat to obtain 40 μm sections, respectively. The sections were pretreated for 20 min with 1% H_2O_2 in PBS containing 0.3% Triton X-100 for inactivation of endogenous peroxidase activity and

permeabilization of cells. The sections were then incubated for 30 min with 5% normal rabbit serum in PBS to block nonspecific protein-binding sites and incubated with anti-WGA polyclonal antibody (1 : 2000, Vector Laboratory, Burlingame, CA), anti-tyrosine hydroxylase (TH) polyclonal antibody (1 : 500, Chemicon, Temecula, CA), anti-BrdU monoclonal antibody (1 : 200, AbD Serotec, UK) in PBS containing 0.3% Triton X-100 with 2% normal rabbit serum overnight at 4℃ and for 2 h at room-temperature. After washing, the sections were incubated with biotin-labeled anti-goat IgG (1 : 200, Vector Laboratory) followed by Vectastatin ABC elite kit (Vector Laboratory), TSA kit (Perkin Almer, Boston, USA) and Vectastatin ABC elite kit again. Signals were visualized with Ni^{2+}-intensified diaminobenzidine/peroxide reaction kit (Vector Laboratory). Specimens were observed with a microscope and computerized digital camera system (Olympus, Tokyo, Japan: Provis), and an image analysis system and program (Adobe Photoshop, San Jose, CA). Evaluation of WGA immunoreactivity levels in various regions of interest was performed as a blind experiment by comparing the stained sections of all mice perfused at different time points in accordance with following criteria[12]: very high (+++), high (++), weak but significant (+), faint (±), or no expression (−) of the WGA transgene product.

In situ hybridization

Sections of formaldehyde-fixed mouse tissues were treated with proteinase K (10 μg/ml at 25℃ for 20 min), acetylated, dehydrated, and air dried. The sections were hybridized for 2 hr at 56℃ in a humidified chamber with DIG-labeled cRNA probe. After hybridization, the sections were washed in 5× SSC, treated with 50% formamide and RNase A (10 μg/ml at 37℃ for 30 min), washed in 2× and 0.2× SSC progressively. The sections were then washed in PBS and incubated with anti-DIG polyclonal antibody (1 : 2000, Roche Diagnostics GmbH, Penzberg, Germany) in PBS with 5% normal rabbit serum. The sections were detected with avidin-Texas Red (Vector Laboratory). The labeled sections were analyzed with a microscope and computerized digital camera system under fluorescent light (Olympus).

BrdU labeling and tissue processing

Cell proliferation was measured by the incorporation of the thymidine analogue 5'-bromo-2-deoxyuridine (BrdU) that is incorporated into the DNA of dividing cells in immunohistochemically detectable quantities during the S phase of cell division.[26] After pFCI, the animals were injected intraperitoneally with BrdU (Roche) (50 mg/kg at a concentration of 10 mg/mL in 0.9% NaCl) and all animals were then sacrificed 4 hours after the BrdU injection.

For immunohistochemical detection of incorporated BrdU, double-stranded DNA was denatured to a single-stranded form suitable for immunohistochemical detection on sections. Sections were incubated in 50% formamide in standard sodium citrate at 65℃ for 2 hr, and treated further with 2 M HCl at 35℃ for 30 min. After being rinsed for 10 min at room temperature in 0.1 M boric acid, the sections were washed with PBS and then incubated with 0.03% H_2O_2 in methanol for 5 min. After having been blocked with the MOM immunodetection kit (Vector Laboratory) according to the standard protocol, the sections were incubated with a primary antibody against BrdU (1 : 1,000, Roche Diagnostics) at room temperature for 30 minutes, washed with PBS, reacted with a biotinylated secondary antibody against mouse IgG (1 : 200) for 10 min at room temperature, and then reacted with streptavidin-biotin-peroxidase complexes for 1hr at room temperature. The peroxidase reaction was visualized by incubation of the sections in diaminobenzidine/hydrogen peroxide solution.

Behavioral assessment

The elevated plus maze was made of black polyvinylchloride and consisted of two opposite open arms (25×5 cm) crossed at right angles with two opposite closed arms of the same size with 25 cm high walls. The arms extended from a central platform (5×5 cm). The maze was elevated to a height of 38.5 cm above the floor level. Mice were placed individually in the center square facing an open arm and allowed to explore the maze for 1 min. An arm entry was counted only when all four paws were inside the arm. Measures scored included: 1) time spent in open arms, 2) time spent in closed arms, 3) number of open arm entries, 4) number of closed arm entries.

Data analysis

The dada were expressed as mean±S.D. The statistical comparisons were performed by unpaired t-test and one-way ANOVA (StatView, SAS Institute, Inc., Cary, NC, USA). The significance between the groups was assigned at $*P<0.05$ and $**P<0.001$.

Results

Adenovirus-mediated WGA expression in LC

In this study, mice were observed at 2 days after viral infection and there was no evidence of cell loss or tissue damage due to the viral infection in LC. In addition, all of the experimental animals that recovered after the infection

remained healthy until being sacrificed without exhibiting any behavioral abnormalities.

Fig. 1A show an adenoviral construct containing WGA gene under control of the eight copies of PRS promoter. All viruses contained the green fluorescent protein (GFP) gene under the control of the CMV promoter, allowing direct observation of viral delivery to the target sites. After injection of PRS-WGA adenovirus to the LC, localization of GFP expression, WGA protein and mRNA was examined on adjacent coronal sections. Colocalization of GFP, TH, and WGA in adjacent sections clearly demonstrated that recombinant adenoviral particles were precisely delivered to TH-expressing NA neuron in the LC and WGA protein was endogenously synthesized in NA neuron of LC (Fig. 1B). In situ hybridization analysis revealed that WGA mRNA was expressed exclusively in LC while no mRNA signal were detected in other sites of brain (Fig. 1C).

Transsynaptic transfer of WGA in noradrenergic neurons of non-injured mice

In sagittal sections of non-injured brain, intense WGA immunoreactivity was detected in the pontine reticular nucleus, motor and sensory trigeminal nucleus, thalamic nucleus, lateral hypothalamic area, deep mesencephalic nucleus, superior colliculus, caudate putamen, corpus callosum, anterior commissure, and olfactory bulb (Fig. 2A). WGA immunoreactivity was also observed in parabrachial nucleus, A5 noradrenergic cells, substantia nigra, lateral habenular nucleus, hippocampus, optic tract, and piriform cortex in coronal sections (Fig. 2B). In the higher magnification field, perikarya were detected in mesencephalic, principal sensory and motor trigeminal nucleus, A5 noradrenergic cells, pontine reticular nucleus, deep mesencephalic nucleus, substantia nigra lateralis, and lateral hypothalamic area (small box in Fig. 2B).

Ischemic brain damage after MCA occlusion

Infarct volume and size measurements from 7 sections of brain (Fig. 3A, B) indicated a significant reduction in lesion size at 8 months after permanent MCA occlusion. Doppler monitoring showed the relative CBF was reduced to 22.6±5.3% of pre-occlusion values within 5 minutes of induction of MCAO in mice (Fig. 3C).

Anatomical changes of noradrenergic circuit after permanent ischemic damage

In acute stage (for first 1 month) after pFCI, noradrenergic circuits containing thalamic area, lateral hypothalamic area, cortex, and hippocampus were destroyed with severe infarction (data not shown). In long-term observation

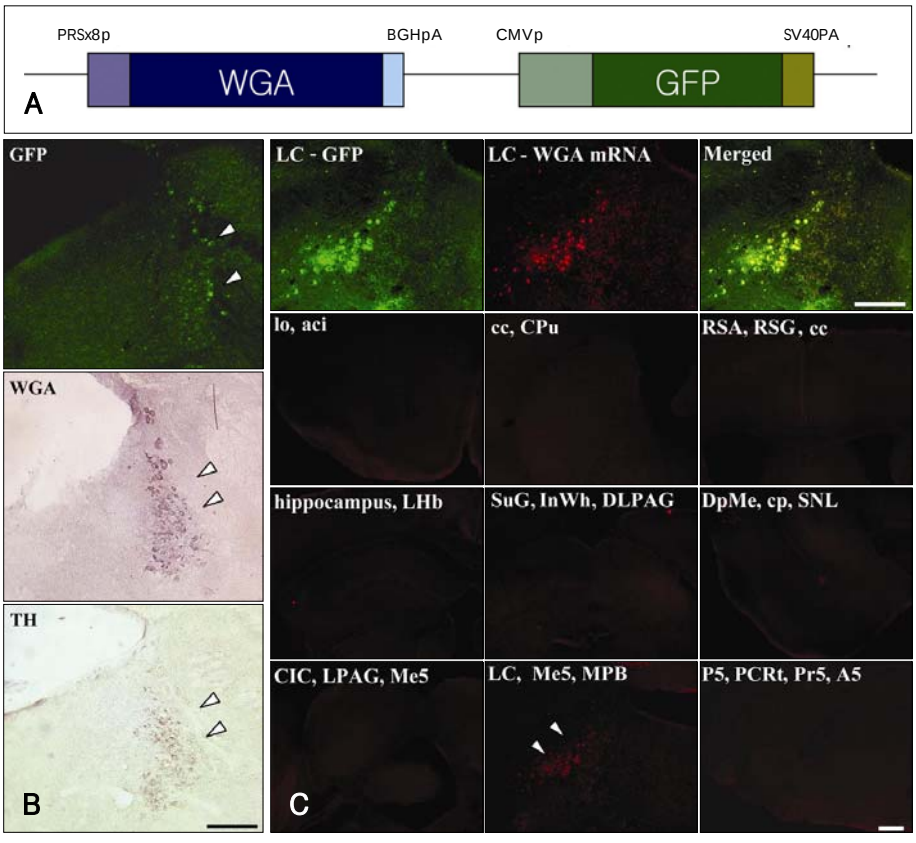

FIGURE 1. Generation and expression of the PRS-WGA adenovirus. A: Schematic diagram indicating the structure of the transgene. B: Adenoviral GFP expression and WGA immunoreactivity were colocalized in TH-positive noradrenergic cell in WGA-adenovirus injected LC. C: In situ hybridization analysis revealed that WGA mRNA was expressed restrictedly in LC neurons. In contrast, no mRNA signal could be detected in other areas of the brain. Scale bar =500 μm.

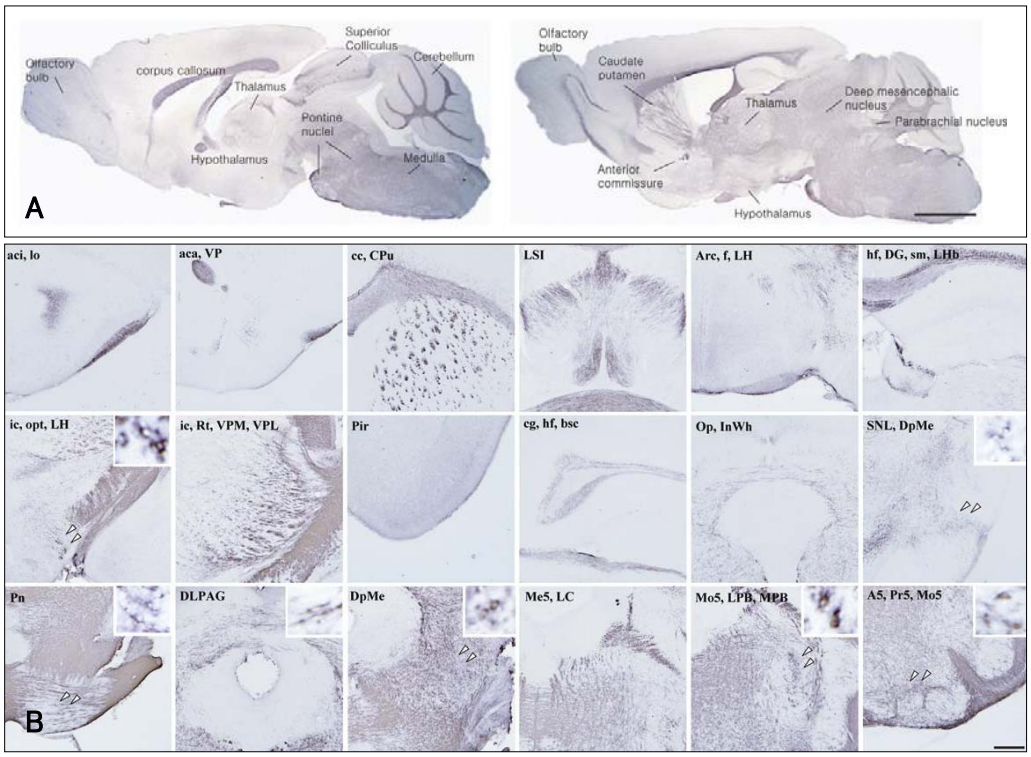

FIGURE 2. WGA immunoreactivity in non-injured mouse brain. After 2 days of PRS-WGA adenovirus injection in LC, LC-originated WGA protein was detected in neurons of several noradrenergic nuclei and other areas. A: Sagittal sections, scale bar=5 mm. B: Coronal sections, scale bar=1 mm.

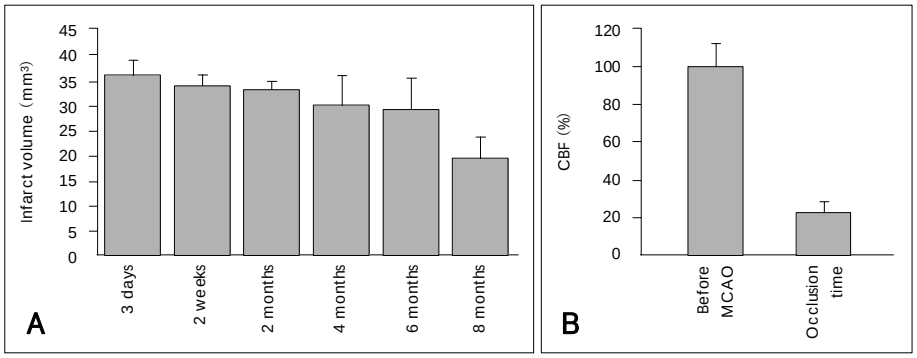

FIGURE 3. Infarct area measurement and regional CBF. A: Lesion volumes had time-dependently reduced after permanent focal cerebral ischemic injury. B: Relative CBF was reduced immediately and continued after pFCI.

(Fig. 4, Table 1), WGA immunoreactivity was not detected in thalamic nucleus, lateral hypothalamic area, hippocampus, amygdaloid nucleus, superior colliculus in ipsilateral hemisphere before 6 months of pFCI onset. In contrast, a very strong WGA immunoreactivity was observed in the contralateral side except for piriform cortex, internal capsule, lateral olfactory tract, optic tract, in undamaged areas of ipsilateral side, and newly recognized in ipsilateral retrosplenial agranular cortex, caudate putamen, mammilothalamic tract, hippocampal fissure, lateral subventricular zone (SVZ), and lateral hypothalamic area. These features indicated that damaged noradrenergic circuits were partly reorganized over time in the area of previous lesion. Especially, hippocampus, thalamic nucleus, lateral hypothalamic area and amygdaloid nucleus were almost completely reorganized at 8 months after pFCI, while WGA immunoreactivity was not detected internal capsule, fornix, piriform cortex, and superior colliculus. More details were showed in Table 1.

BrdU labeling

Widespread BrdU immunopositive cells were observed in the postischemic corpus callosum, thalamic areas, hypothalamic areas, and hippocampus ipsilateral to the ischemic infarct at 1 month and 6 months after pFCI (Fig. 5). BrdU-positive cells were more frequently observed in the ipsilateral SVZ than the contralateral side. At 1 month after pFCI, many BrdU immunopositive cells were detected in the le-

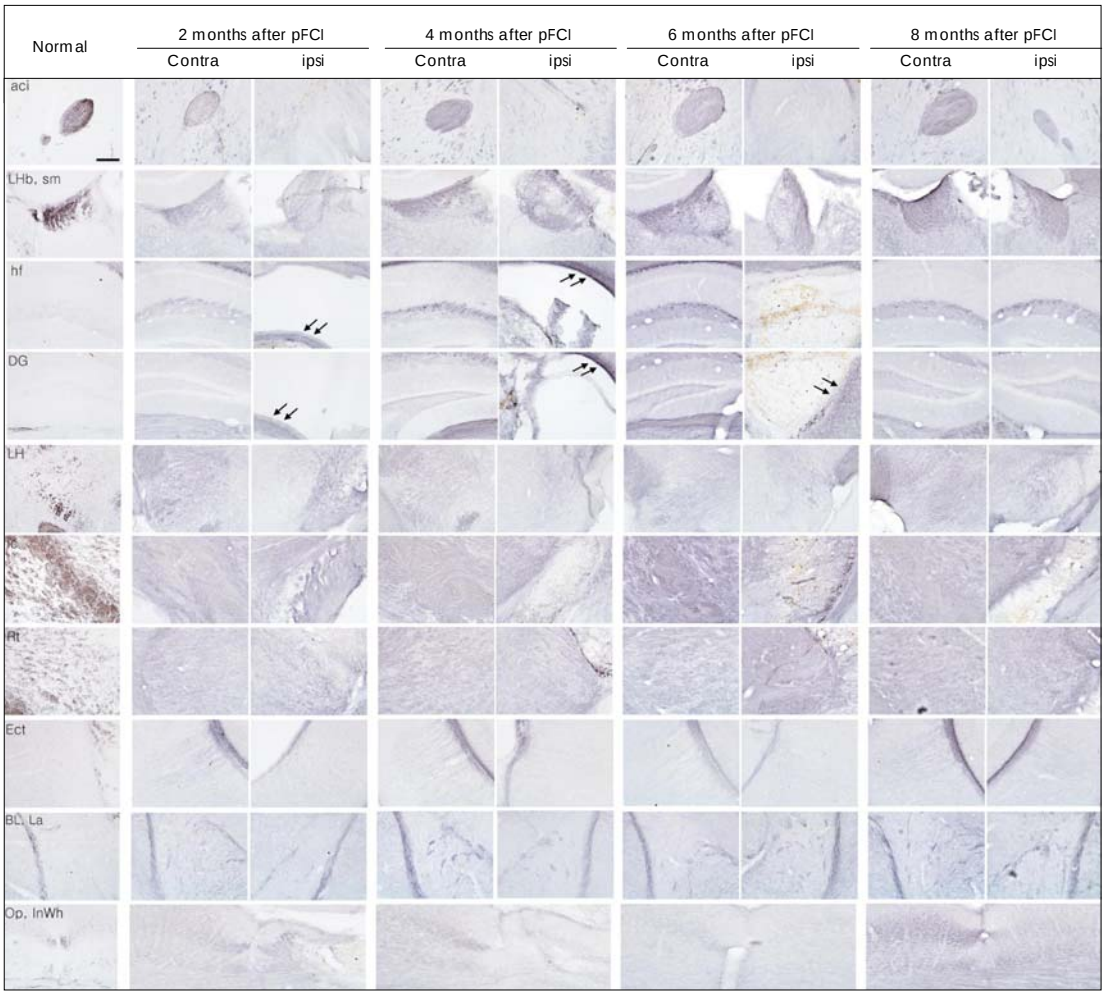

FIGURE 4. WGA immunoreactivity after pFCI. The WGA positive-neurons were not detected in lesion sites within 6 months after ischemic injury, whereas reorganized WGA positive cells were newly found in several lesioned sites except for internal capsule and superior colliculus at 8 months after pFCI. Scale bar=500 μm.

sioned thalamus and hypothalamus, and many BrdU positive fusiform-shaped nuclei suggesting migrating cells were also observed in SVZ and corpus callosum of both hemispheres. At 6 months after pFCI, the incidence of BrdU positive cells in the ipsilateral thalamus and hypothalamus was significantly diminished compared to that of 1month after pFCI. No BrdU immunolabeling was detected in contralateral side, except for SVZ and corpus callosum.

Neurological outcome and physiological parameters

The mean arterial blood pressure (MABP) increased gradually to peak at 4 months after pFCI and then gradually returned to that of baseline at 8 months (preocclusion value: 83.6±3.7 mmHg; 4 months value after MCAO: 95.4±5.4 mmHg, $*P<0.01$; 8 months value after MCAO: 87.4±6.2 mmHg) (Fig. 6A).

The body temperature and weight were also monitored at several time points after pFCI in daylight cycle (Fig. 6B, C). The body temperature was significantly lower than that of sham-operation at all time points by 6 months after ischemic injury (within a week after sham-operation: 37.5±0.6℃, after pFCI: 35.8±0.9℃, $*P=0.002$; 1 month- sham: 38.0±0.3℃, -pFCI: 36.7±0.6℃, $**P<0.001$; 2 months-sham: 38.2±0.5℃, -pFCI: 36.7±0.3℃, $**P<0.001$; 4 months-sham: 38.0±0.2℃, -pFCI: 36.9±0.4℃, $**P<0.001$; 6 months-sham: 37.9±0.2℃, -pFCI: 37.1±0.3℃, $*P=0.003$). However it also returned close that of the baseline sham-operation value at 8 months (8 months-sham: 37.8±0.4℃, -pFCI: 37.3±0.2℃). The mean weight of pFCI groups was shown also to recover gradually in time-dependent manner. At the first 1 month after ischemic injury, the mean weight of pFCI groups was significantly lower than that of sham-operation groups (within a week-sham: 23.3±0.9 g, -pFCI: 19.2±2.4 g, $**P<0.001$; 1 month-sham: 25.7±1.7 g, -pFCI: 23.6±1.9 g, $*P=0.004$), which was returned nearly to the sham-operation value at 2 months.

Thereafter it had reduced again and stabilized at the significantly lower value until 8 months (8 months-sham: 34.5 ±2.3 g, -FCI: 29.9±3.6 g, $^{**}P<0.001$). This inconsistent result in 8 months after pFCI may caused by the influence of other factors such as aging.

Elevated plus maze test

To assess the role of NA in anxiety-like behavior, mice were subjected to elevated plus maze tests at several time points after pFCI (Table 2). At 2 months after pFCI, mice spent a significantly more time on the open arms of the

TABLE 1. WGA expression in whole brain 2 days after PRS-WGA adenovirus injection in pFCI induced mice

WGA immune-reactive site	Normal	2 month		4 month		6 month		8 month	
		Contra	ipsi	Contra	Ipsi	Contra	Ipsi	Contra	ipsi
aci	++	++	−	++	−	++	−	++	+
lo	++	+	+	+	+	++	++	++	++
VP	++	++	+	++	++	++	++	++	++
LSl	++	++	+	++	+	++	+	++	++
Cg2	−	+	+	+	−	+	−	+	+
LHb, sm	++	++	+	++	+	++	+	++	++
hf	±	+	−	++	−	++	−	++	++
DG	±	+	−	++	−	++	−	++	++
RSA	++	++	+++	++	++	++	++	++	++
LH	++	++	+	++	±	++	±	++	++
mt	+++	++	++	++	++	++	+	++	++
Opt	+++	++	−	++	−	++	+	++	+
ic	+++	++	+	++	−	++	−	++	−
f	++	++	+	++	±	++	−	++	±
Rt	++	++	+	++	±	++	+	++	++
Ect	±	++	−	++	−	++	+	++	+
Pir	++	−	−	−	−	−	−	±	±
BL, La	±	++	±	++	+	++	++	++	++
Op	+	+	−	++	−	++	−	+++	−
InWh	±	+	−	+	−	±	−	++	++
DpMe	++	++	++	++	+	++	+	++	++
Me5	++	++	++	++	−	+	−	++	++
DRV	−	++	−	+	−	−	−	−	−

+++: very high, ++: high, +: weak, ±: faint, −: no expression

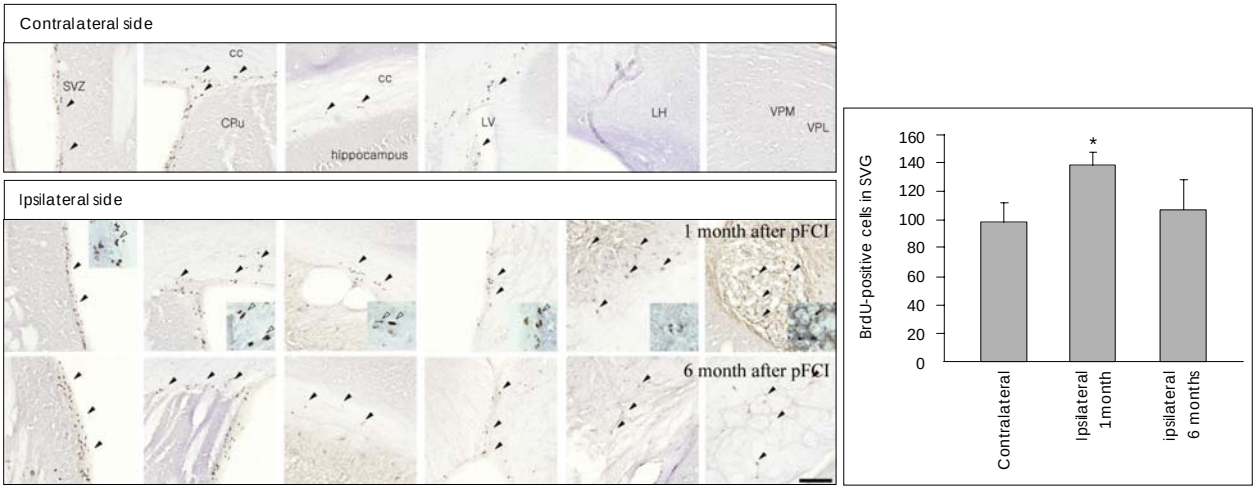

FIGURE 5. Detection of migrated and differentiated endogenous precursor cells. BrdU positive cells were detected in SVZ and corpus callosum in both hemisphere and increased in SVZ, thalamic, and hypothalamic areas in ipsilateral side at 1 month and 6 months (black arrow). BrdU positive fugiform-shaped nuclei were also observed in SVZ and cc (white arrow). Semi-quantitative histogram shows the number of BrdU-positive cells in subventricular zone. *p<0.05. Scale bar=100 μm.

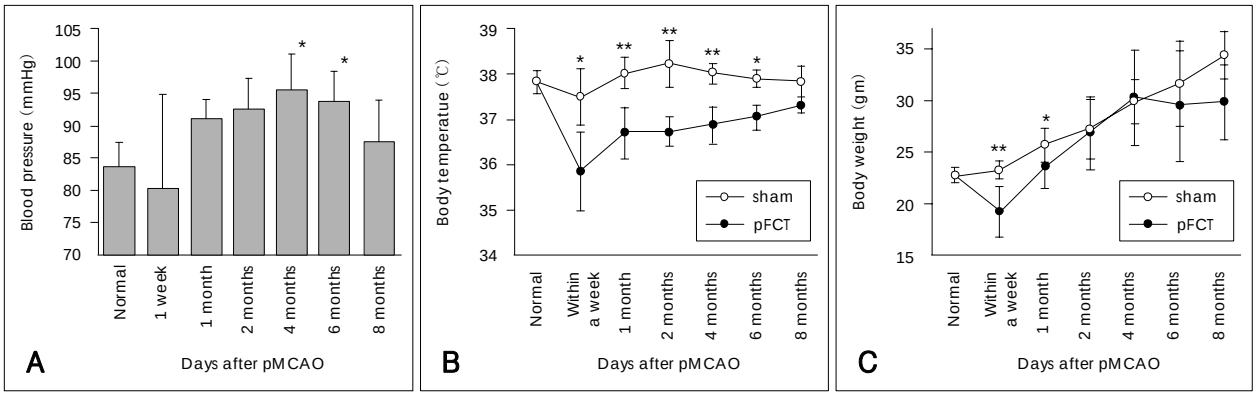

FIGURE 6. Evaluation of physiological recovery related anatomical reorganization. Temporally, a significant improvement in (A) blood pressure, (B) body temperature, and (C) Body weight were observed after excessive functional failure with ischemic injury. This improvement was shown especially from 6 months after pFCI and physiological functions were returned to normal level nearly at 8 months.

TABLE 2. Summary of behavioral measures on the elevated plus-maze following pFCI

Behavioral data	Within a week		1 month		2 months		4 months		6 months	
	sham	pFCI	sham	pFCI	sham	pFCI	sham	pFCI	sham	pFCI
Time spent in open arms (s)	2.2±1.5	11.0±2.3**	7.6±2.9	14.7±4.0*	10.4±2.4	14.9±3.2*	12.0±3.7	9.7±5.6	5.3±1.0	8.6±4.8
Time spent in closed arms (s)	51.4±5.0	30.0±9.5*	31.2±8.7	26.8±8.0	36.6±8.9	29.6±7.1	32.3±3.4	36.3±8.8	26.3±8.7	37.4±6.7*
Number of open arm entries (times)	1.0±0.7	0.3±0.6	1.6±0.9	1.4±1.1	1.2±0.8	1.2±1.1	2.5±0.6	1.8±1.0	1.8±0.5	2.7±1.1
Number of closed arm entries (times)	2.4±1.5	1.3±0.6	2.6±0.9	2.2±1.3	2.2±0.4	2.4±0.9	3.3±1.3	3.3±1.0	3.3±1.5	3.1±1.5

Values are mean±STD. Significant difference from sham group by student' t-test. *P<0.05, **P<0.001

plus maze than sham-operated mice and the number of open arms entry was also higher in pFCI mice than sham-operated mice, which were returned to that of control mice by 6 month after pFCI. The number of closed arms entry and the time stayed on the closed arms were not significant different. These data suggested that pFCI conferred anxiolytic effects to mice initially but gradually dissipated over time upon the recovery of neurological deficits and the reorganization of NA circuitry.

Discussion

This study demonstrated the feasibility of transsynaptic labeling by using WGA-expressing adenoviral vector in the mouse noradrenergic system. By simply injecting the virus solution into the unilateral LC, the noradrenergic neural pathways were clearly visualized with great accuracy and high reproducibility from LC to its projectional areas in this study (Fig. 2). An early work using horseradish peroxidase in rat[27] demonstrated a topographic organization within the LC nucleus such that cells projecting to hippocampus and septum were located in the dorsal LC, those projecting to cerebellum were in both dorsal and ventral LC, and those projecting to the thalamus and hypothalamus were in the caudal and rostral poles. Later work showed that cortically-projecting LC neurons were more prominent within the caudal portion of nucleus and these neurons projected in a predominantly ipsilateral (>95%) manner.[28] In contrast to this previous study, symmetric bilateral projections to both hemispheres were shown in this study.

Compared to the conventional method in which WGA protein was injected into target sites, present method successfully and reliably detected more strong transsynaptically transferred WGA protein, which might be related to efficient infection of adenovirus to the noradrenergic neurons as well as promoter elements (PRS promoter) being used for robust expression of WGA. PRS has previously been shown to be an NA-specific cis element binding to paired-like homeodomain factor Phox2a/Phox2b.[29] It has been confirmed that increasing copies of PRS cause synergistic activation of reporter gene expression reaching maximal efficacy at eight copies. An adenoviral construct containing eight copies of PRS was shown to induce strong expression of β-galactosidase in NA neurons upon its microinjection to LC,[25] which was in agreement with successful visualization of NA system in mouse brain with recombinant adenoviral

vector expressing WGA under the control of PRS promoter elements in this study (Fig. 1). Moreover, in higher magnification field, the observation of perikarya in remote areas from LC indicates that WGA protein underwent the anterograde transsynaptic transfer from LC. It was previously reported that WGA proteins appear in granule-like structures in neurons, bind to N-acetylglucosamine and sialic acid in carbohydrate moiety of glycoproteins and glycolipids expressed on neuronal surface plasma membrane, are efficiently taken up into neurons by endocytosis, and are transported through axons and dendrites.[17] Similar appearance of WGA in neurons in the present study suggests that, following the synthesis and maturation in LC, WGA transgene product underwent the same endocytotic, secretory, and transfer pathways.

It has also successfully demonstrated the process of reorganization of NA circuitries after pFCI in a time-dependent manner in the present study. Intense WGA immunoreactivity was initially detected in the most contralateral side and the ipsilateral non-lesioned areas, which was followed by subsequent appearance in several areas of infarction by pFCI, such as thalamic nucleus, lateral hypothalamic area, lateral habenular nucleus, and amygdala. These findings suggest that compensatory reinforcement of undamaged ipsilateral sites and contralateral NA circuits occurred shortly after the onset of pFCI and then evolved into subsequent reorganization of NA circuitries in severely damaged area. The recovery and reorganization of neural circuitries in the lesion may be mediated by compensatory sproutings of neuronal processes in intact areas as well as novel endogenous repair strategy in injured spinal cord of adult rat.[23,30]

Recently, a comprehensive review of data obtained from PET, fMRI and transcranial magnetic stimulation methods supports the general hypothesis that clinical recovery after a stroke is associated with increased neuronal activities in non-injured brain areas.[31] In this study, it was interesting to find strong WGA immunoreactivity never seen in non-injured mice in the hippocampal fissure and SVZ at the edge of damaged hippocampus, which was not seen in non-injured mice after pFCI (Fig. 4, black arrow). It has been found that an acute stroke induced by MCAO precipitates cellular proliferation or neurogenesis in the ipsilateral SVZ and a large number of immature neurons migrate from SVZ to ipsilateral infracted areas at 2 weeks following insults.[32,33] The strong WGA immunoreactivity in the hippocampus and adjacent SVZ in present study may represent those newly proliferated, migrating neurons executing a crucial role in the recovery of damaged area after pFCI. To confirm this hypothesis, BrdU immunohistochemistry, a thymidine analogue, was used at 1 month and 6 month after pFCI (Fig. 5). BrdU is incorporated into the proliferating cell nuclei during the S-phase of a cell cycle for DNA duplication and has been widely used to explore neural stem cell proliferation in the central nervous system.[26]

It was also known that brain insults such as cerebral ischemia, causing neuronal death, are accompanied by increased neurogenesis in the SGZ and SVZ.[34,35] BrdU positive cells were observed in thalamic and hypothalamic lesions, increased BrdU positive cells in SVZ, and fusiform-shaped nuclei in SVZ and corpus callosum, which was consistent with the process of initial neuronal proliferation in SVZ and their subsequent migration into the ischemic lesions as a repair mechanism.

To assess the relationship of remodeling process with functional recovery in NA system, the alteration of blood pressure, body temperature, weight, and behavior was investigated on several time points after pFCI (Fig. 6). In this study, data showed that the gradual recovery of blood pressure, body temperature, body weight, and behavior following acute infarction was closely related with the anatomical reorganization of hypothalamus, thalamus, and amygdala at 6 month of pFCI. Dysfunction of the NA system has been widely known to be associated with alterations of blood pressure,[4,36] body temperature,[37,38] and weight,[39] and anxiety.[5,40] Previous experiments indicated that blood pressure was significantly higher in mice having insular infarction.[4,36] Insular cortex is directly connected with central nucleus of the amygdala and the posterior lateral hypothalamus[41,42] belonging to NA system. Although WGA immunoreactivity was not detected in the insular cortex in this study, it was speculated that the lateral hypothalamus, amygdala, and parabrachial nucleus are directly connected with insular cortex and the circuitry damage is responsible for the dysfunction and recovery of blood pressure.

Early studies also found that lesions of hypothalamic nucleus or thalamic nucleus resulted in alterations of body temperature and body weight in models of MPTP-neurotoxicity in pFCI, ischemic injury, and stereotaxic injury.[37,38,43] In line with these studies, the present results seem to explain that the altered physiological dysfunction precipitated by acute insults in above anatomical structures may gradually recover as the reorganization processes of damaged NA systems mature in those structures. As shown in Table 2, using the elevated plus maze, significant reduction was found in anxiety-like behavior in a time-dependent manner with the anatomical changes following pFCI, as displayed by an increase in time spent on the open arms. The locomotor activity of animals, represented by the number of closed arms entries, was not significantly different between sham-operation and pFCI group.

Therefore, a decrease in anxiety is independent of any changes in locomotor activity. Increase in NA signaling is associated with hightened anxiety and decrease in NA signaling is related with less anxiety. Central administration of adrenergic antagonists or lesions of the locus coeruleus in rats reduced anxiogenic effects in the elevated plus maze.[44,45] The results of present study are again in agreement with initial dysfunction of NA activities and following its gradual recovery over time along with reorganization of NA circuits in the infracted structures.

In conclusion, the results were successfully visualized the circuitries of noradrenergic system in mice by using transsynaptic tracing with PRS-WGA adenovirus and confirmed the phenomenon of reorganization of damaged NA circuitries before and after pFCI. Moreover, there were close temporal relationships between the physiological and functional recovery and the reorganization of damaged NA circuits. The process of reorganization may involve axonal sprouting of intact NA projections making synapses on newly proliferated and migrated neurons to the infarct area, which require further clarification by additional studies. In addition, this study has provided evidence that the WGA-expressing adenoviral vector system using cell-type specific promoter is an extremely valuable tool for the investigations of formation, refinement, maintenance, and remodeling of neural networks as well as their functional implications.

REFERENCES

1. Silver FL, Norris JW, Lewis AJ, Hachinski VC. Early mortality following stroke: a prospective review. *Stroke* 1984;15:492-96.
2. Myers MG, Norris JW, Hachniski VC, Sole MJ. Plasma norepinephrine in stroke. *Stroke* 1981;12:200-4.
3. Tokgozoglu SL, Batur MK, Top uoglu MA, Saribas O, Kes S, Oto A. Effects of stroke localization on cardiac autonomic balance and sudden death. *Stroke* 1999;30:1307-11.
4. Smith KE, Hachinski VC, Gibson CJ, Ciriello J. Changes in plasma catecholamine levels after insula damage in experimental stroke. *Brain Res* 1986;375:182-5.
5. Marino MD, Bourdelat-Parks BN, Cameron Liles L, Weinshenker D. Genetic reduction of noradrenergic function alters social memory and reduces aggression in mice. *Behav Brain Res* 2005;161:197-203.
6. Marcin MS, Nemeroff CB. The neurobiology of social anxiety disorder: the relevance of fear and anxiety. *Acta Psychiatr Scand Suppl* 2003:51-64.
7. Sander D, Winbeck K, Klingelhofer J, Etgen T, Conrad B. Prognostic relevance of pathological sympathetic activation after acute thromboembolic stroke. *Neurology* 2001;57:833-8.
8. Cechetto DF. Identification of a cortical site for stress-induced cardiovascular dysfunction. *Integr Physiol Behav Sci* 1994;29:362-73.
9. Cechetto DF, Chen SJ. Subcortical sites mediating sympathetic responses from insular cortex in rats. *Am J Physiol* 1990;258:R245-55.
10. Hallett M. Plasticity of the human motor cortex and recovery from stroke. *Brain Res Brain Res Rev* 2001;36:169-74.
11. Rijntjes M, Weiller C. Recovery of motor and language abilities after stroke: the contribution of functional imaging. *Prog Neurobiol* 2002;66:109-22.
12. Kinoshita N, Mizuno T, Yoshihara Y. Adenovirus-mediated WGA gene delivery for transsynaptic labeling of mouse olfactory pathways. *Chem Senses* 2002;27:215-23.
13. Yoshihara Y. Visualizing selective neural pathways with WGA transgene: combination of neuroanatomy with gene technology. *Neurosci Res* 2002;44:133-40.
14. Yoshihara Y, Mizuno T, Nakahira M, Kawasaki M, Watanabe Y, Kagamiyama H, et al. A genetic approach to visualization of multisynaptic neural pathways using plant lectin transgene. *Neuron* 1999;22:33-41.
15. Gonatas NK, Harper C, Mizutani T, Gonatas JO. Superior sensitivity of conjugates of horseradish peroxidase with wheat germ agglutinin for studies of retrograde axonal transport. *J Histochem Cytochem* 1979;27:728-34.
16. Itaya SK. Anterograde transsynaptic transport of WGA-HRP in rat olfactory pathways. *Brain Res* 1987;409:205-14.
17. Fabian RH, Coulter JD. Transneuronal transport of lectins. *Brain Res* 1985;344:41-8.
18. Itaya SK, van Hoesen GW. WGA-HRP as a transneuronal marker in the visual pathways of monkey and rat. *Brain Res* 1982;236:199-204.
19. Lee HS, Kim MA, Waterhouse BD. Retrograde double-labeling study of common afferent projections to the dorsal raphe and the nuclear core of the locus coeruleus in the rat. *J Comp Neurol* 2005;481:179-93.
20. Byrum CE, Guyenet PG. Afferent and efferent connections of the A5 noradrenergic cell group in the rat. *J Comp Neurol* 1987;261:529-42.
21. Hanno Y, Nakahira M, Jishage K, Noda T, Yoshihara Y. Tracking mouse visual pathways with WGA transgene. *Eur J Neurosci* 2003;18:2910-4.
22. Sugita M, Shiba Y. Genetic tracing shows segregation of taste neuronal circuitries for bitter and sweet. *Science* 2005;309:781-5.
23. Bareyre FM, Kerschensteiner M, Raineteau O, Mettenleiter TC, Weinmann O, Schwab ME. The injured spinal cord spontaneously forms a new intraspinal circuit in adult rats. *Nat Neurosci* 2004;7:269-77.
24. Vakili A, Kataoka H, Plesnila N. Role of arginine vasopressin V1 and V2 receptors for brain damage after transient focal cerebral ischemia. *J Cereb Blood Flow Metab* 2005;25:1012-9.
25. Hwang DY, Carlezon WA Jr, Isacson O, Kim KS. A high-efficiency synthetic promoter that drives transgene expression selectively in noradrenergic neurons. *Hum Gene Ther* 2001;12:1731-40.
26. Reynolds BA, Weiss S. Generation of neurons and astrocytes from isolated cells of the adult mammalian central nervous system. *Science* 1992;255:1707-10.
27. Mason ST, Fibiger HC. Regional topography within noradrenergic locus coeruleus as revealed by retrograde transport of horseradish peroxidase. *J Comp Neurol* 1979;187:703-24.
28. Waterhouse BD, Lin CS, Burne RA, Woodward DJ. The distribution of neocortical projection neurons in the locus coeruleus. *J Comp Neurol* 1983;217:418-31.
29. Yang C, Kim HS, Seo H, Kim CH, Brunet JF, Kim KS. Paired-like homeodomain proteins, Phox2a and Phox2b, are responsible for noradrenergic cell-specific transcription of the dopamine beta-hydroxylase gene. *J Neurochem* 1998;71:1813-26.
30. Bareyre FM, Haudenschild B, Schwab ME. Long-lasting sprouting and gene expression changes induced by the monoclonal antibody IN-1 in the adult spinal cord. *J Neurosci* 2002;22:7097-110.
31. Rossini PM, Calautti C, Pauri F, Baron JC. Post-stroke plastic reorganisation in the adult brain. *Lancet Neurol* 2003;2:493-502.
32. Arvidsson A, Collin T, Kirik D, Kokaia Z, Lindvall O. Neuronal replacement from endogenous precursors in the adult brain after stroke. *Nat Med* 2002;8:963-70.
33. Kokaia Z, Lindvall O. Neurogenesis after ischaemic brain insults. *Curr Opin Neurobiol* 2003;13:127-32.
34. Jiang W, Gu W, Brannstrom T, Rosqvist R, Wester P. Cortical neurogenesis in adult rats after transient middle cerebral artery occlusion. *Stroke* 2001;32:1201-7.

35. Jin K, Minami M, Lan JQ, Mao XO, Batteur S, simon RP, et al. Neurogenesis in dentate subgranular zone and rostral subventricular zone after focal cerebral ischemia in the rat. *Proc Natl Acad Sci USA* 2001;98:4710-5.
36. Meyer S, Strittmatter M, Fischer C, Georg T, Schmitz B. Lateralization in autonomic dysfunction in ischemic stroke involving the insular cortex. *Neuroreport* 2004;15:357-61.
37. Corbett D, Thornhill J. Temperature modulation (hypothermic and hyperthermic conditions) and its influence on histological and behavioral outcomes following cerebral ischemia. *Brain Pathol* 2000;10: 145-52.
38. Moy LY, Albers DS, Sonsalla PK. Lowering ambient or core body temperature elevates striatal MPP+ levels and enhances toxicity to dopamine neurons in MPTP-treated mice. *Brain Res* 1998;790:264-9.
39. King BM. The rise, fall, and resurrection of the ventromedial hypothalamus in the regulation of feeding behavior and body weight. *Physiol Behav* 2006;87:221-44.
40. Pandaranandaka J, Poonyachoti S, Kalandakanond-Thongsong S. Anxiolytic property of estrogen related to the changes of the monoamine levels in various brain regions of ovariectomized rats. *Physiol Behav* 2006;87:828-35.
41. Mufson EJ, Mesulam MM, Pandya DN. Insular interconnections with the amygdala in the rhesus monkey. *Neuroscience* 1981;6:1231-48.
42. Saper CB. Convergence of autonomic and limbic connections in the insular cortex of the rat. *J Comp Neurol* 1982;210:163-73.
43. Marien MR, Colpaert FC, Rosenquist AC. Noradrenergic mechanisms in neurodegenerative diseases: a theory. *Brain Res Brain Res Rev* 2004;45:38-78.
44. Cecchi M, Khoshbouei H, Morilak DA. Modulatory effects of norepinephrine, acting on alpha 1 receptors in the central nucleus of the amygdala, on behavioral and neuroendocrine responses to acute immobilization stress. *Neuropharmacology* 2002;43:1139-47.
45. Lapiz MD, Mateo Y, Durkin S, Parker T, Marsden CA. Effects of central noradrenaline depletion by the selective neurotoxin DSP-4 on the behaviour of the isolated rat in the elevated plus maze and water maze. *Psychopharmacology (Berl)* 2001;155:251-9.

– Appendix –

Abbreviations			
A5	A5 noradrenaline cells	LHb	lateral habenular nucleus
aca	anterior commissure, anterior part	lo	lateral olfactory tract
aci	anterior commissure, intrabulbar part	LPAG	lateral periaqueductal gray
Arc	arcuate hypothalamic nucleus	LPB	lateral parabrachial nucleus
BL	basolateral amygdaloid nucleus	LSl	lateral septal nucleus, intermediate part
bsc	brachium of the superior colliculus	Me5	mesencephalic trigeminal nucleus
cc	corpus callosum	mlf	medial longitudinal fasciculus
cg	cingulum	Mo5	motor trigeminal nucleus
Cg2	cingulate cortex, area 2	MPB	medial parabrachial nucleus
CIC	central nucleus of the inferior colliculus	Op	optic nerve layer of the superior colliculus
cp	cerebral peduncle, basal part	opt	optic tract
CPu	caudate putamen	P5	peritrigeminal zone
DG	dentate gyrus	PCRt	parvicellular reticular nucleus
DLPAG	dorsolateral periaqueductal gray	Pir	piriform cortex
DpMe	deep mesencephalic nucleus	Pn	pontine nuclei
DRV	dorsal raphe nucleus, ventral part	Pr5	principal sensory trigeminal nucleus
f	fornix	RSA	retrosplenial agranular cortex
hf	hippocampal fissure	RSG	retrosplenial granular cortex
ic	internal capsule	Rt	reticular thalamic nucleus
InG	intermediate gray layer of the superior colliculus	sm	stria medullaris of the thalamus
InWh	intermediate white layer of the superior colliculus	SNL	substantia nigra, lateral part
La	lateral amygdaloid nucleus	SuG	superficial gray layer of the superior colliculus
LC	locus coeruleus	VP	ventral pallidum
LH	lateral hypothalamic area	VPL	ventral posterolateral thalamic nucleus
		VPM	ventral posteromedial thalamic nucleus